(Preprint) AAS 17-270

# HYBRID GUIDANCE CONTROL FOR A HYPERVELOCITY SMALL SIZE ASTEROID INTERCEPTOR VEHICLE

**Melak M. Zebenay*, Joshua R. Lyzhoft†, and Brent W. Barbee‡**

Near-Earth Objects (NEOs) are comets and/or asteroids that have orbits in proximity with Earth's own orbit. NEOs have collided with the Earth in the past, which can be seen at such places as Chicxulub crater, Barringer crater, and Manson crater, and will continue in the future with potentially significant and devastating results. Fortunately such NEO collisions with Earth are infrequent, but can happen at any time. Therefore it is necessary to develop and validate techniques as well as technologies necessary to prevent them. One approach to mitigate future NEO impacts is the concept of high-speed interceptor. This concept is to alter the NEO's trajectory via momentum exchange by using kinetic impactors as well as nuclear penetration devices. The interceptor has to hit a target NEO at relative velocity which imparts a sufficient change in NEO velocity. NASA's Deep Impact mission has demonstrated this scenario by intercepting Comet Temple 1, 5 km in diameter, with an impact relative speed of approximately 10 km/s. This paper focuses on the development of hybrid guidance navigation and control (GNC) algorithms for precision hypervelocity intercept of small sized NEOs. The spacecraft's hypervelocity and the NEO's small size are critical challenges for a successful mission as the NEO will not fill the field of view until a few seconds before intercept. The investigation needs to consider the error sources modeled in the navigation simulation such as spacecraft initial state uncertainties in position and velocity. Furthermore, the paper presents three selected spacecraft guidance algorithms for asteroid intercept and rendezvous missions. The selected algorithms are classical Proportional Navigation (PN) based guidance that use a first order difference to compute the derivatives, Three Plane Proportional Navigation (TPPN), and the Kinematic Impulse (KI). A manipulated Bennu orbit that has been changed to impact Earth will be used as a demonstrative example to compare the three methods. In addition, a hybrid approach that is a combination between proportional navigation and kinematic impulse will be investigated to find an effective, error tolerant, and power saving approach. A 3-dimension mission scenario for both the asteroid and the interceptor spacecraft software simulator is developed for testing of the controllers. The current result demonstrates that a miss distance magnitude of less than 10m is found using the PN and TPPN guidance laws for small asteroid in the presence of error in the spacecraft states. Moreover, the paper presents these results and also the hybrid control approach simulation results.

## INTRODUCTION

The investigation focuses on the development of advanced Guidance Navigation and Control (GNC) algorithms for precision hypervelocity intercept of small size Near-Earth Objects (NEOs). NEOs are asteroids and comets whose orbits approach or cross Earth's orbit.

*NASA Postdoctoral Researcher, Solar System Exploration Division, Melak.m.zebenay@nasa.gov, AIAA Member, OAK Ridge Institute for Science and Education, Oak Ridge, TN, 37831, USA.

†Student Trainee, Navigation and Mission Design Branch, NASA, Iowa State University, Ames, Iowa, 50011, USA.

‡Ast, Aerospace Veh Design & MSN Analyst, Navigation and Mission Design Branch, NASA, NASA Goddard Space Flight Center, Greenbelt, Maryland, 20770, USA.

The goal of this investigation is to suggest the optimal GNC algorithm for a given target NEO and as well as for spacecraft components (i.e. sensors and spacecraft thrusters etc.). Hypervelocity intercept speeds and the NEO's small size are critical challenges for a successful mission, as the NEO will not fill the Field of View until a few seconds before intercept. The investigation needs to consider the error sources modeled in the navigation simulation such as spacecraft initial state uncertainties of in position and in velocity, 3-axis spacecraft attitude uncertainty, and random centroid pixel noise with bias. This report presents three selected spacecraft guidance algorithms for asteroid intercept and rendezvous missions.[1,2] The selected algorithms are classical proportional navigation (PN)[3] based guidance that uses a first order difference to compute the derivatives,[4] Three Plane Proportional Navigation (TPPN)[5] and the kinematic Impulse (KI).[1,4,6] These algorithms are implemented in software and tested using a specific mission scenario example.

## TERMINAL GUIDANCE, NAVIGATION AND CONTROL SUBSYSTEM

The Asteroid Intercept mission will end with a terminal intercept guidance phase that requires execution of guided trajectory correction maneuvers to compensate for errors in orbital navigation of the target asteroid. This phase starts after the on-board sensors acquire the target asteroid states. For example, for a small target asteroid (50 to 100m) the terminal phase might start 2 hours prior to intercept, but for larger asteroid or comet it might comparatively start much earlier.

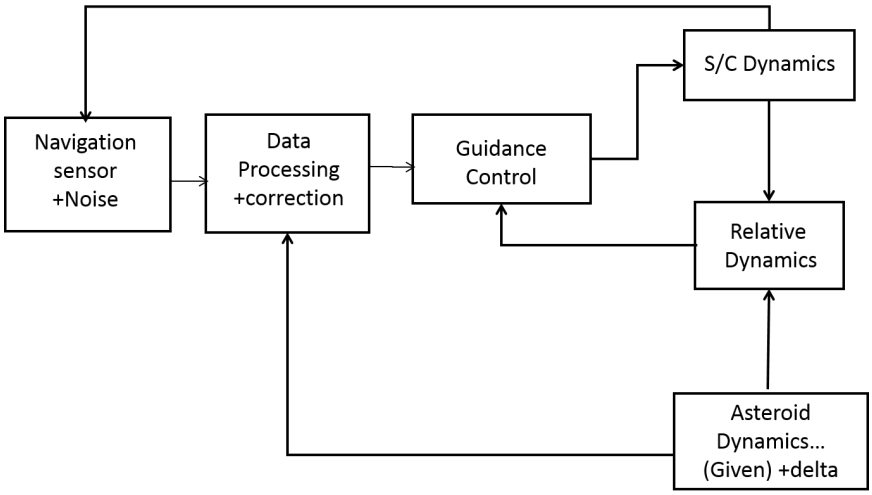


**Figure 1. Block diagram of asteroid Intercept GNC concept.**

The Terminal Guidance, Navigation, and Control (GNC) subsystem is one of the key subsystems of the Asteroid intercept and rendezvous mission. Figure 1 presents a block diagram for the Asteroid Intercept GNC concept that is modeled in simulation to emulate the asteroid intercept mission scenarios. GNC must be done autonomously based on on-board measurements of the asteroid states as commanding from Earth via a communications link would otherwise introduce a time-delay that will not be tolerated for hypervelocity asteroid intercept missions.

In order to implement the GNC concepts, first the dynamics simulator of the asteroid and spacecraft is developed and implemented into software. The GNC is presented in the next section. Figure 2 gives a graphical representation of the vectors related to the asteroid and spacecraft with respect to the sun.

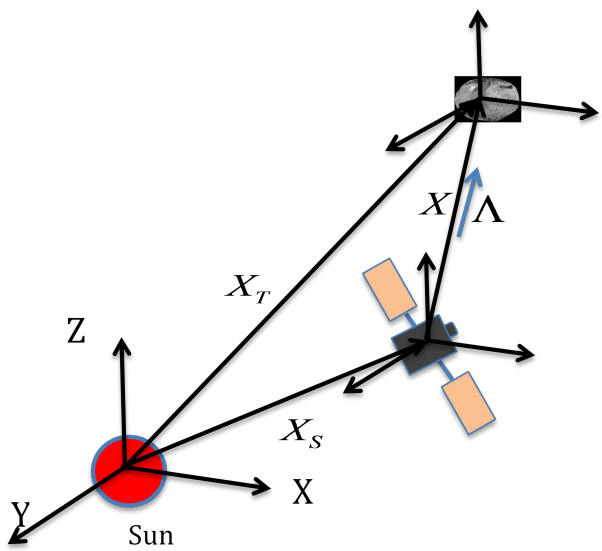


**Figure 2. Asteroid intercept and rendezvous geometry.**

The target asteroid is modeled as a point mass in standard heliocentric Keplerian Orbit, as follows:

$$\dot{\mathbf{x}}_T = \frac{d}{dt}\mathbf{x}_T \tag{1}$$

$$\ddot{\mathbf{x}}_T = \mathbf{g}_T \tag{2}$$

$$\mathbf{g}_T = -\frac{\mu_\odot \mathbf{x}_T(t)}{\|\mathbf{x}_T(t)\|_2^3} \tag{3}$$

where $\mathbf{x}_T$ is the position vector of asteroid with respect to the sun frame, $\mu_\odot$ is the solar gravitational parameter, and $\mathbf{g}_T$ is the gravitational acceleration due to the sun.
Similarly, the dynamics of the spacecraft is derived as:

$$\dot{\mathbf{x}}_S = \frac{d}{dt}\mathbf{x}_S \tag{4}$$

$$\ddot{\mathbf{x}}_S = \mathbf{g}_S \tag{5}$$

$$\mathbf{g}_S = -\frac{\mu_\odot \mathbf{x}_S(t)}{\|\mathbf{x}_S(t)\|_2^3} + \mathbf{u}(t) \tag{6}$$

where $\mathbf{x}_S$ is the position vectors of the spacecraft with respect to the sun frame, $\mathbf{g}_S$ is the gravitational acceleration acting on the spacecraft due to the sun, and $\mathbf{u}$ is the control acceleration provided by the spacecraft thrusters. Other disturbing acceleration is neglected due to the assumption of small size asteroid.[1]

The relative position of the spacecraft with respect to the target asteroid is computed as:

$$\mathbf{x}_R = \mathbf{x}_S - \mathbf{x}_T \tag{7}$$

$$\dot{\mathbf{x}}_R = \frac{d}{dt}\mathbf{x}_S - \frac{d}{dt}\mathbf{x}_T \tag{8}$$

$$\ddot{\mathbf{x}}_R = \mathbf{g}_S - \mathbf{g}_T \tag{9}$$

## SPACECRAFT INTERCEPT GUIDANCE CONTROLLERS

It requires continued investigation of different terminal-phase guidance laws for each mission scenario due to the difference in the mission requirements and spacecraft capabilities as well as the target asteroid parameters. This section reviews three guidance controllers, which are proportional navigation (PN) guidance, Three-plane proportional navigation (TPPN) and kinematic impulse (KI).

### Proportional Navigation (PN)

The PN guidance law commands acceleration, perpendicular to the instantaneous spacecraft-asteroid line-of-sight. The acceleration commands are proportional to the line-of-sight rate and closing velocity. The guidance law can be stated as:[3]

$$\mathbf{u} = n v_c \dot{\boldsymbol{\lambda}} \tag{10}$$

where $\mathbf{u}$ is the control acceleration command, n is a unitless effective navigation gain (usually in the range of 3-5), $v_c$ is the spacecraft-asteroid closing velocity, and $\dot{\lambda}$ is the line-of-sight rate.

The closing velocity, time to go, and the line-of-sight rate is computed as follow:

$$v_c = -\dot{\mathbf{x}}_R \cdot \boldsymbol{\lambda} \tag{11}$$

$$\delta t = \frac{\|\mathbf{x}_R\|_2}{v_c} \tag{12}$$

$$\boldsymbol{\lambda}(t) = -\frac{\mathbf{x}_R(t)}{\|\mathbf{x}_R(t)\|_2} \tag{13}$$

$$\dot{\boldsymbol{\lambda}} = \frac{d\boldsymbol{\lambda}}{dt} \approx \frac{\boldsymbol{\lambda}(t) - \boldsymbol{\lambda}(t - \delta t)}{\delta t} \tag{14}$$

### Three Plane Proportional Navigation (TPPN)

The three-plane approach for 3D true proportional navigation was designed for a missile to target intercept,[5] which is adapted for spacecraft to asteroid intercept in this report. The TPPN method projects the spacecraft-asteroid relative motion onto xy, xz and yz perpendicular planes and then solves the problem in each plane independently for two-dimensional proportional navigation. Then the method produces a 3D solution by combining these 2D solutions. Figure 3 shows the three-dimensional engagement space projected onto three perpendicular planes: xy, xz and yz. From Figure 3, the 3D solution are derived by combining the components of 2D solutions and equations. The line of sight (LOS) angles:

$$\lambda_{xy} = \tan^{-1}\left(\frac{y_R}{x_R}\right) \tag{15}$$

$$\lambda_{xz} = \tan^{-1}\left(\frac{z_R}{x_R}\right) \tag{16}$$

$$\lambda_{yz} = \tan^{-1}\left(\frac{z_R}{y_R}\right) \tag{17}$$

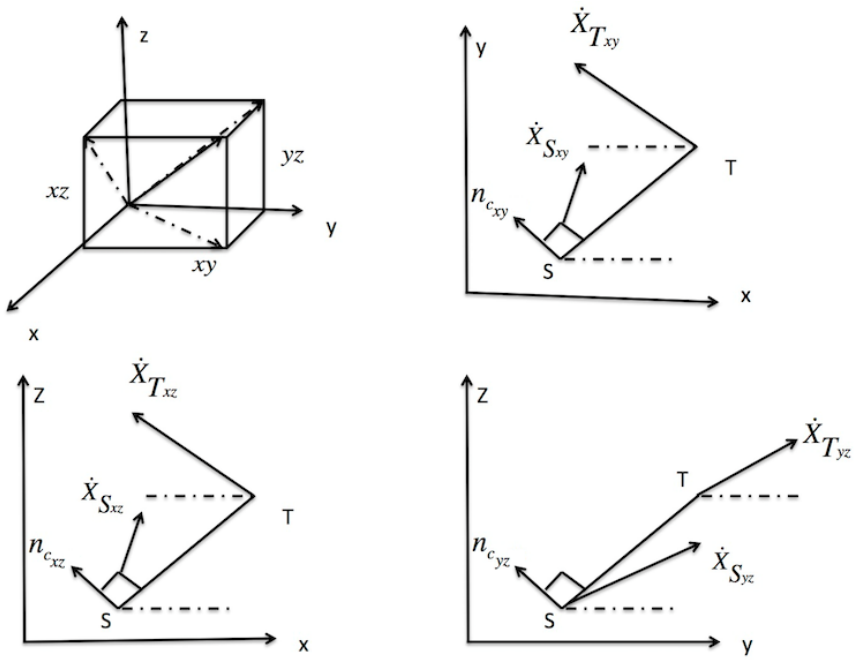


**Figure 3. Projections of Spacecraft Relative state vector onto Three Planes (xy, xz and yz).**

where $x_R$, $y_R$, and $z_R$ are the position components of the relative state vector, $\mathbf{x}_R$. Line of sight rates for each plane are found to be:

$$\dot{\lambda}_{xy} = \frac{x_R\dot{y}_R - y_R\dot{x}_R}{x_R^2 + y_R^2} \tag{18}$$

$$\dot{\lambda}_{xz} = \frac{x_R\dot{x}_R - z_R\dot{x}_R}{x_R^2 + z_R^2} \tag{19}$$

$$\dot{\lambda}_{yz} = \frac{y_R\dot{z}_R - z_R\dot{y}_R}{y_R^2 + z_R^2} \tag{20}$$

where $\dot{x}_R$, $\dot{y}_R$, and $\dot{z}_R$ are the velocity components of the relative state vector, $\mathbf{x}_R$. The closing velocities for each plane are computed as:

$$v_{c_{xy}} = -\frac{x_R\dot{x}_R + y_R\dot{y}_R}{\sqrt{x_R^2 + y_R^2}} \tag{21}$$

$$v_{c_{xz}} = -\frac{x_R\dot{x}_R + z_R\dot{z}_R}{\sqrt{x_R^2 + z_R^2}} \tag{22}$$

$$v_{c_{yz}} = -\frac{y_R\dot{y}_R + z_R\dot{z}_R}{\sqrt{y_R^2 + z_R^2}} \tag{23}$$

Hence, the acceleration commands for each plane are derived as follow:

$$n_{c_{xy}} = m\dot{v}_{c_{xy}}\dot{\lambda}_{xy} \tag{24}$$

$$n_{c_{xz}} = m\dot{v}_{c_{xz}}\dot{\lambda}_{xz} \tag{25}$$

$$n_{c_{yz}} = m\dot{v}_{c_{yz}}\dot{\lambda}_{yz} \tag{26}$$

where $m$ is the effective navigation ratio and is bounded by:

$$3\frac{\|\dot{\mathbf{x}}_S\|_2 - \|\dot{\mathbf{x}}_T\|_2}{\|\dot{\mathbf{x}}_S\|_2} < m < 3\frac{\|\dot{\mathbf{x}}_S\|_2 + \|\dot{\mathbf{x}}_T\|_2}{\|\dot{\mathbf{x}}_S\|_2} \tag{27}$$

The spacecraft guidance command for each axis can be computed by combining two commands that share the same axis. Thus, the components of acceleration command in each axis is derived as follow:

$$\ddot{x}_S = -n_{c_{xy}}\sin(\lambda_{xy}) - n_{c_{xz}}\sin(\lambda_{xz}) \tag{28}$$

$$\ddot{y}_S = n_{c_{xy}}\cos(\lambda_{xy}) - n_{c_{yz}}\sin(\lambda_{yz}) \tag{29}$$

$$\ddot{z}_S = n_{c_{xz}}\cos(\lambda_{xz}) + n_{c_{yz}}\cos(\lambda_{yz}) \tag{30}$$

Collecting each component yields the control command calculated by TPPN and is given in the controal acceleration vector:

$$\mathbf{u} = [\ddot{x}_S \quad \ddot{y}_S \quad \ddot{z}_S] \tag{31}$$

**Kinematic Impulse (KI) Guidance**

KI guidance control method is a predictive control approach. It is based on the estimation of the line of sight and takes into account the target's future position. The method depends on a linearized theory to minimize the cost of on-board computations. Predictive guidance requires on-board measurement to estimate the line-of-sight, as well as line-of-sight rate, and knowledge of the target asteroid's orbit. This will also be represented by the relative error state transition matrix, which is derived from orbit perturbation theory.[7] A reference target represented by the asteroid's state, $\mathbf{x}_T^*$, is used to determine the spacecraft state, $\mathbf{x}_S$, with the incorporation of the perturbation, $\delta\mathbf{x}$. This expression is

$$\mathbf{x}_S = \mathbf{x}_T^* + \delta\mathbf{x} \tag{32}$$

were $\mathbf{x}_T^*$ is the reference target and is given by

$$\mathbf{x}_T^* = [x_T \quad y_T \quad z_T \quad \dot{x}_T \quad \dot{y}_T \quad \dot{z}_T]^T \tag{33}$$

For simplicity, the magnitude of the reference target position vector is given by

$$r_T = \sqrt{x_T^2 + y_T^2 + z_T^2} \tag{34}$$

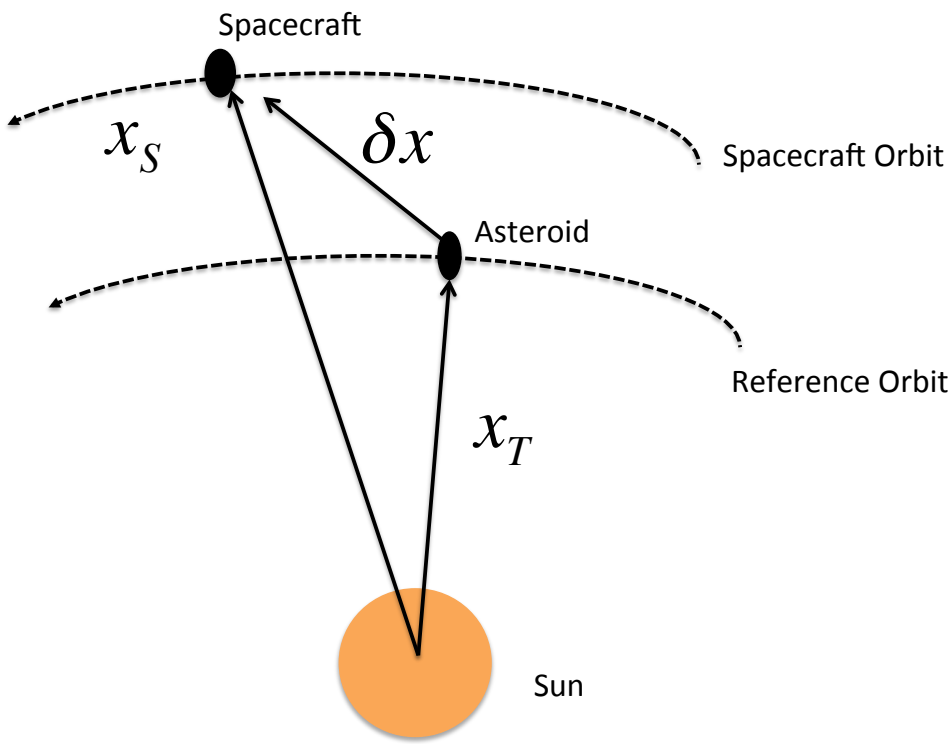


**Figure 4. Target Asteroid and Spacecraft perturbation geometry**

In general, by using the spacecraft state, the differential motion equation can be written as follow:

$$\dot{\mathbf{x}}_S = \mathbf{f}\left(\mathbf{x}_S, t\right) = \begin{bmatrix} \dot{x}_S \\ \dot{y}_S \\ \dot{z}_S \\ \ddot{x}_S \\ \ddot{y}_S \\ \ddot{z}_S \end{bmatrix} = \begin{bmatrix} f_1 \\ f_2 \\ f_3 \\ f_4 \\ f_5 \\ f_6 \end{bmatrix} = \begin{bmatrix} \dot{x}_S \\ \dot{y}_S \\ \dot{z}_S \\ -\frac{\mu_\odot \, x_S}{r_S^3} \\ -\frac{\mu_\odot \, y_S}{r_S^3} \\ -\frac{\mu_\odot \, z_S}{r_S^3} \end{bmatrix} \tag{35}$$

where $\mathbf{x}_S$ is the magnitude of the spacecraft's positions vector. By using equation 35 and substituting in equation 32, the equations of motion using the perturbed theory is

$$\dot{\mathbf{x}}_T = \mathbf{f}\left(\mathbf{x}_T, t\right) = \mathbf{f}\left(\mathbf{x}_T^* + \delta\mathbf{x}, t\right) \tag{36}$$

Then by expanding the nonlinear equation using a Taylor series expansion about $\mathbf{x}_T^*$ and incorporating the time derivative of equation 32 as well as applying reference trajectory state knowledge at any given time, the perturbed differential equation is

$$\delta\dot{\mathbf{x}}(t) = \mathbf{F}(t)\,\delta\mathbf{x}(t) \tag{37}$$

where $\mathbf{F}$ is the Jacobian of the $\mathbf{f}$ vector which is evaluated at $\mathbf{x}_T^*$. This expression is defined by

$$\mathbf{F}(t) = \left[\frac{\partial \mathbf{f}(t)}{\partial \mathbf{x}(\mathbf{t})}\right]_* = \begin{bmatrix} 0 & 0 & 0 & 1 & 0 & 0 \\ 0 & 0 & 0 & 0 & 1 & 0 \\ 0 & 0 & 0 & 0 & 0 & 1 \\ -\frac{\mu_\odot}{r_T^3} + \frac{3\mu_\odot x_T^2}{r_T^5} & \frac{3\mu_\odot x_T y_T}{r_T^5} & \frac{3\mu_\odot x_T z_T}{r_T^5} & 0 & 0 & 0 \\ \frac{3\mu_\odot y_T x_T}{r_T^5} & -\frac{\mu_\odot}{r_T^3} + \frac{3\mu_\odot y_T^2}{r_T^5} & \frac{3\mu_\odot y_T z_T}{r_T^5} & 0 & 0 & 0 \\ \frac{3\mu_\odot z_T x_T}{r_T^5} & \frac{3\mu_\odot z_T y_T}{r_T^5} & -\frac{\mu_\odot}{r_T^3} + \frac{3\mu_\odot z_T^2}{r_T^5} & 0 & 0 & 0 \end{bmatrix}_* \tag{38}$$

By expanding the state error equation, equation 32, using a Taylor series as well as substituting in equation 37 along with its time derivatives, the expression for the evolution of the state error, given an initial state and change in time, can be written as

$$\delta\mathbf{x} = \left[\mathbf{I} + \mathbf{F}(t)\delta t + \frac{1}{2}\mathbf{F}(t)^2\delta t^2 + ...\right]\delta\mathbf{x}_o = \mathbf{\Phi}\delta\mathbf{x}_o \tag{39}$$

where $\mathbf{I}$ is a 6x6 identity matrix, $\delta\mathbf{x}_o$ is the initial relative or state error state, $\delta t$ is the change in time from the initial state to the final desired state, and $\mathbf{\Phi}$ is the state transition matrix. Recall, this is used for the evolution of the relative/orbit error state. The state transition matrix used for estimating the relative state is given by

$$\mathbf{\Phi} = \begin{bmatrix} 1+\frac{3\mu_\odot x_T^2\delta t^2}{2\mathbf{x}_T^5}-\frac{\mu_\odot\delta t^2}{2\mathbf{x}_S^3} & \frac{3\mu_\odot y_T y_T\delta t^2}{2\mathbf{r}_S^5} & \frac{3\mu_\odot x_T z_T\delta t^2}{2\mathbf{r}_T^5} & \delta t & 0 & 0 \\ \frac{3\mu_\odot x_T y_T\delta t^2}{2\mathbf{r}_T^5} & 1+\frac{3\mu_\odot y_T^2\delta t^2}{2\mathbf{r}_T^5}-\frac{\mu_\odot\delta t^2}{2\mathbf{r}_T^3} & \frac{3\mu_\odot y_T z_T\delta t^2}{2\mathbf{r}_T^5} & 0 & \delta t & 0 \\ \frac{3\mu_\odot x_T z_T\delta t^2}{2\mathbf{r}_T^5} & \frac{3\mu_\odot y_T z_T\delta t^2}{2\mathbf{r}_T^5} & 1+\frac{3\mu_\odot z_T^2\delta t^2}{2\mathbf{r}_T^5}-\frac{\mu_\odot\delta t^2}{2\mathbf{r}_T^3} & 0 & 0 & \delta t \\ \frac{-\mu_\odot\delta t}{r^3}+\frac{3\mu_\odot x_T^2\delta t}{\mathbf{r}_T^5} & \frac{3\mu_\odot x_T y_T\delta t}{\mathbf{r}_T^5} & \frac{3\mu_\odot x_T z_T\delta t}{\mathbf{r}_T^5} & 1+\frac{3\mu_\odot x_T^2\delta t^2}{2\mathbf{r}_T^5}-\frac{\mu_\odot\delta t^2}{2\mathbf{r}_T^3} & \frac{3\mu_\odot x_T y_T\delta t^2}{2\mathbf{r}_T^5} & \frac{3\mu_\odot x_T z_T\delta t^2}{2\mathbf{r}_T^5} \\ \frac{3\mu_\odot x_T y_T\delta t}{\mathbf{r}_T^5} & \frac{-\mu_\odot\delta t}{\mathbf{r}_T^3}+\frac{3\mu_\odot y_T^2\delta t}{\mathbf{r}_T^5} & \frac{3\mu_\odot y_T z_T\delta t}{\mathbf{r}_T^5} & \frac{3\mu_\odot x_T y_T\delta t^2}{2\mathbf{r}_T^5} & 1+\frac{3\mu_\odot y_T^2\delta t^2}{2\mathbf{r}_T^5}-\frac{\mu_\odot\delta t^2}{2\mathbf{r}_T^3} & \frac{3\mu_\odot y_T z_T\delta t^2}{2\mathbf{r}_T^5} \\ \frac{3\mu_\odot z_T x_T\delta t}{\mathbf{r}_T^5} & \frac{3\mu_\odot y_T z_T\delta t}{\mathbf{r}_T^5} & \frac{-\mu_\odot\delta t}{\mathbf{r}_T^3}+\frac{3\mu_\odot z_T^2\delta t}{\mathbf{r}_T^5} & \frac{3\mu_\odot x_T \mathbf{r}_T\delta t^2}{2\mathbf{r}_T^5} & \frac{3\mu_\odot z_T z_T\delta t^2}{2\mathbf{r}_T^5} & 1+\frac{3\mu_\odot z_T^2\delta t^2}{2\mathbf{r}_T^5}-\frac{\mu_\odot\delta t^2}{2\mathbf{r}_T^3} \end{bmatrix} \tag{40}$$

where $\delta t$ is the time to go, $x_T$, $y_T$, and $z_T$ are the position components for the asteroid, and $r_T$ is the magnitude of the asteroid's position vector. However, for simplification, the state transition matrix, $\mathbf{\Phi}$, will be set into four 3x3 matrices. This is denoted by

$$\mathbf{\Phi} = \begin{bmatrix} \mathbf{\Phi}_1 & \mathbf{\Phi}_2 \\ \mathbf{\Phi}_3 & \mathbf{\Phi}_4 \end{bmatrix} \tag{41}$$

The expression for the relative position at a final time given an initial relative position is

$$\mathbf{x}\left(t_f\right) \approx \tilde{\mathbf{x}}_{t_f} = \mathbf{\Phi}_1(t)\mathbf{x}(t) + \mathbf{\Phi}_2(t)\dot{\mathbf{x}}(t) \tag{42}$$

The unit vector for the estimated final state vector is written as

$$\boldsymbol{\lambda}_c = \frac{\tilde{\mathbf{x}}t_f}{\|\tilde{\mathbf{x}}t_f\|_2} \tag{43}$$

Since the predicted final relative position is calculated, the needed change in velocity can be estimated. It is assumed that the relative velocity of the spacecraft and asteroid has a very small change. By doing so, the needed approximated change in velocity is found to be

$$\delta\mathbf{v} = \frac{\tilde{\mathbf{x}}_{t_f}}{\|\tilde{\mathbf{x}}_{t_f}\|_2} v_c - \tilde{\mathbf{v}} \tag{44}$$

where $\tilde{\mathbf{v}}$ is the approximation of the relative velocity. The expression for $\tilde{\mathbf{v}}$ can be found by using the state transition matrix or estimated by using a combination of the line of sight and line of sight rate. By using the latter, the expression for the estimation for the relative velocity is

$$\tilde{\mathbf{v}} = -v_c \delta t \dot{\boldsymbol{\lambda}}(t) - v_c \boldsymbol{\lambda}(t) \tag{45}$$

By substituting equations 43 and 45 into equation 44, the final approximation for the change in velocity is found to be

$$\delta\mathbf{v} = v_c \left( \boldsymbol{\lambda}_c + \delta t \dot{\boldsymbol{\lambda}}(t) + \boldsymbol{\lambda}(t) \right) \tag{46}$$

With the required change in velocity estimated, the command acceleration may also be found. What must be commanded is along the same unit vector as the change in velocity and can then be written as

$$\mathbf{u} = T_{max} \frac{\delta\mathbf{v}}{\|\delta\mathbf{v}\|_2} \tag{47}$$

where $T_{max}$ is the maximum amount of thrust available by the guidance system. Further details on the state transition matrix and velocity change derivations can be found in.[1,7]

## RESULTS

In order to evaluate the performance of the guidance controllers presented in this paper, simulation software called Hypervelocity Intercept Guidance Simulator (HIGS) was implemented. Each object and controller, the spacecraft, asteroid and guidance controllers, were developed as independent modules that can be integrated as required. The HIGS software was implemented using Matlab Simulink. Figure 5 shows the schematics of the software implementation of the dynamics and the guidance controllers.

A manipulated Bennu orbit that has been changed to impact Earth was used as a demonstrative example to compare the PN, TPPN, KI, KI/PN hybrid, and KI/TPPN hybrid. Orbit states were given one day prior to Asteroid intercept and at the intercept time. The asteroid has a mass of 523598775.598299 kilograms. In addition, the perturbed states of the spacecraft one day prior to the Asteroid intercept were also given. This data was used to initialize the dynamics of asteroid and spacecraft, which was updated for each sampling time. The results presented in this section are based on the given data as shown in Table 1 and using HIGS.

The guidance controllers presented in this document were implemented and used the in house developed HIGS software. While using standard heliocentric Keplerian orbits, the spacecraft and asteroid were assumed to be point masses. Each guidance controller was applied two hours before estimated intercept or miss time. HIGS was initialized with a fixed-step sampling time of 0.01 seconds and was propagated using a 4$^{\text{th}}$-order Runge-Kutta numerical integration scheme. In the absence of guidance controller, the assumed initial parameters will result in a miss distance of approximately 5.46 kilometers. The implemented controllers were applied two hour before the intercept of the target asteroid.

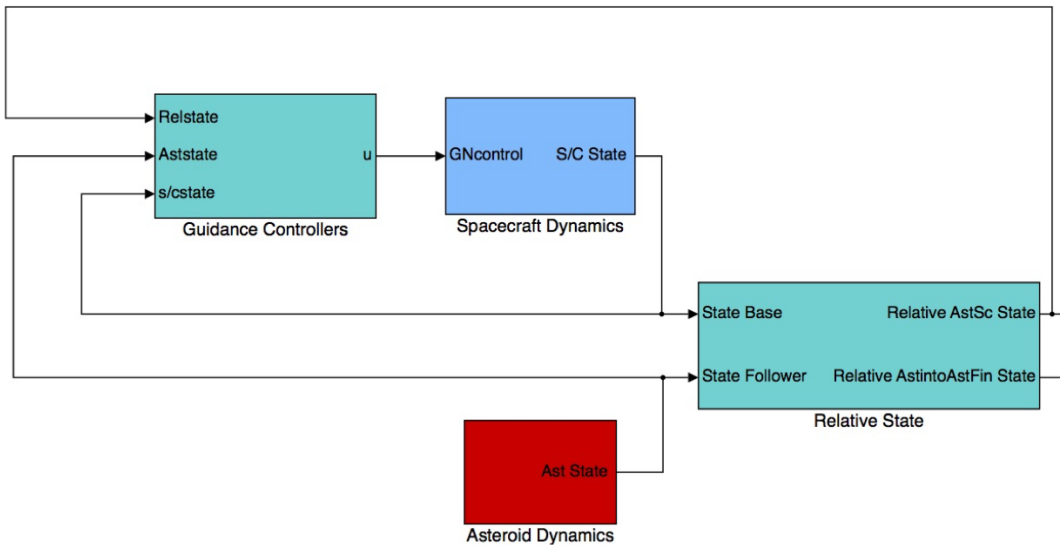


**Figure 5. Schematics of the HIGS software Simulator**

Figure 6 shows the computed required commands, relative position magnitude between the spacecraft and asteroid Bennu for PN controller. If the continuous control commands could be implemented successfully, the PN controller demonstrates that it would cause a miss distance of approximately 6.649 meters. This controller is directly proportional to line-of-sight which is computed by finite differencing. The finite differencing caused non-smooth acceleration commands as shown in the right half of Figure 6. Improvements to the PN guidance response might be seen by implementing a smoothing filtering.

Figure 7 contains subplots which describe the computed spacecraft change in velocity as well as relative position magnitude corresponding the the TPPN implementation. The TPPN controller demonstrated an improvement compared to the uncontrolled case. This improvement was shown by decreasing the minimum miss distance from to approximately 11.4 meters. By varying the effective navigation ratio, m, the miss error can be improved. Unlike PN controller TPPN controller, as shown in the right side of Figure 7, have smooth command accelerations.

By implementing preplanned maneuver times, KI guidance can be used to deliver the necessary firing commands corresponding to each time, if the estimated spacecraft velocity change is greater that what is allowed by the thrusters. Figure 8 presents the computed desired commands, relative position magnitude between the spacecraft and asteroid Bennu for KI controller. The KI controller demonstrated an improvement compared to both uncontrolled case and TPPN controller with a miss

| Body stats | x [km] | y[km] | z[km] | x [km/s] | y[km/s] | z[km/s] |
|---|---|---|---|---|---|---|
| Asteroid-Bennu's Orbit | -35005191.005 | 133007414.776 | 14545381.55 | -33.091 | 5.293 | 5.293 |
| Perturbed spacecraft | 35242510.768 | 132933523.539 | 14427507.779 | -30.345 | -30.345 | 0.776 |

**Table 1. The given initial conditions one day prior to Asteroid Intercept**

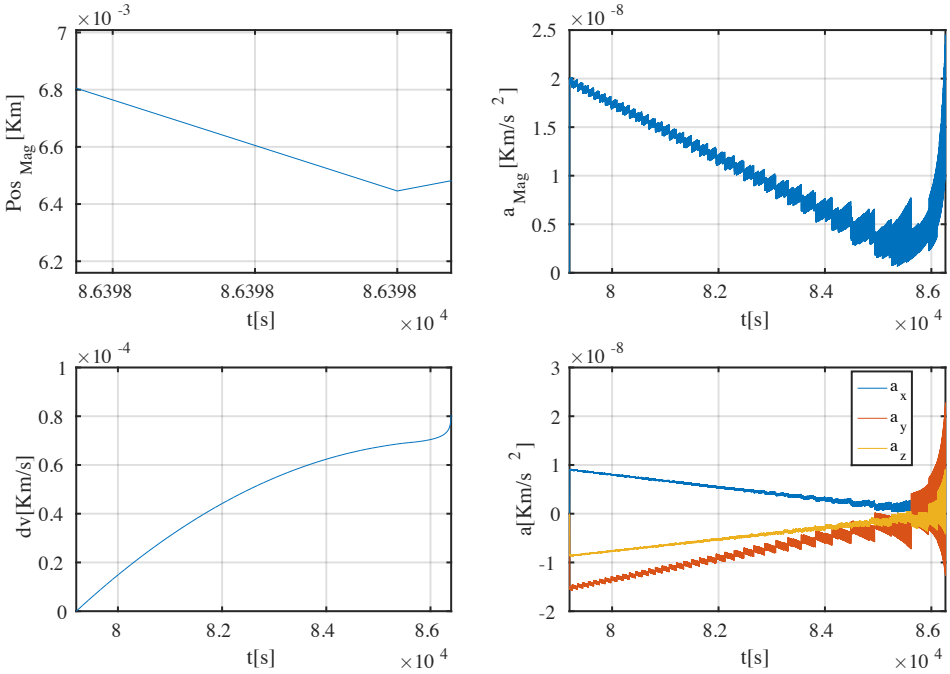


**Figure 6. PN Controller profile: Position magnitude vs. time (top left), Commanded acceleration magnitude vs. time (top right), Total dv usage vs. time(bottom left), and applied accelerations of PN guidance law applied to an asteroid intercept problem (bottom right)**

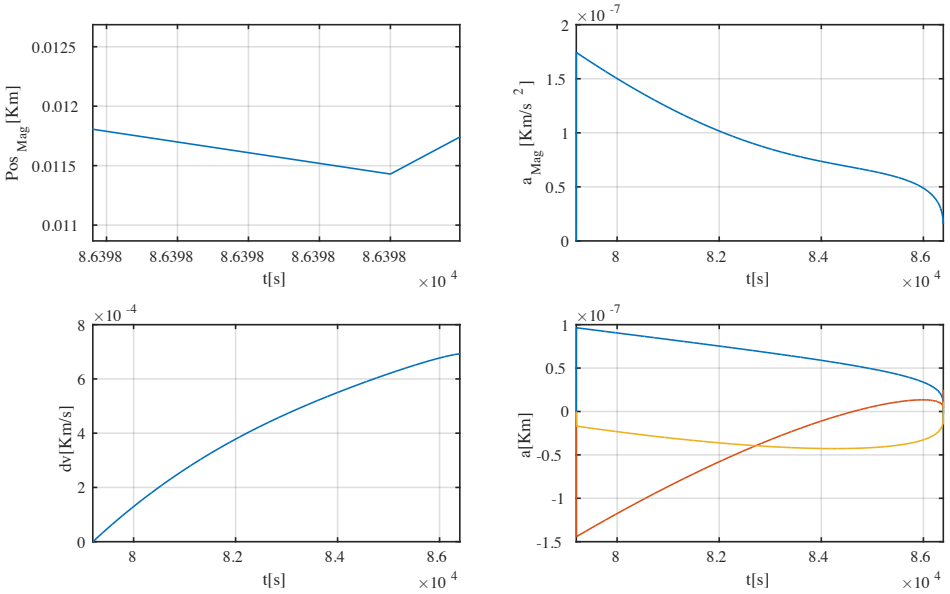


**Figure 7. TPPN Controller profile: position magnitude vs. time (top left), Commanded acceleration magnitude vs. time (top right), dv usage vs. time(bottom left), and Applied accelerations of PN guidance law applied to an asteroid intercept problem (bottom right)**

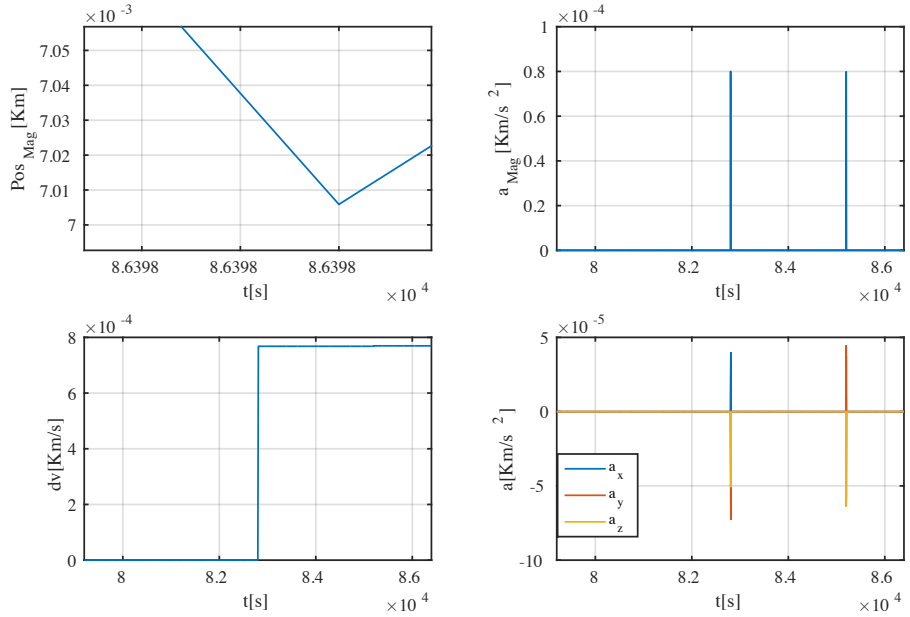


**Figure 8. KI Controller profile: Position magnitude vs. time (top left), Commanded acceleration magnitude vs. time (top right), Total dv usage vs. time(bottom left), and Applied accelerations of PN guidance law applied to an asteroid intercept problem (bottom right)**

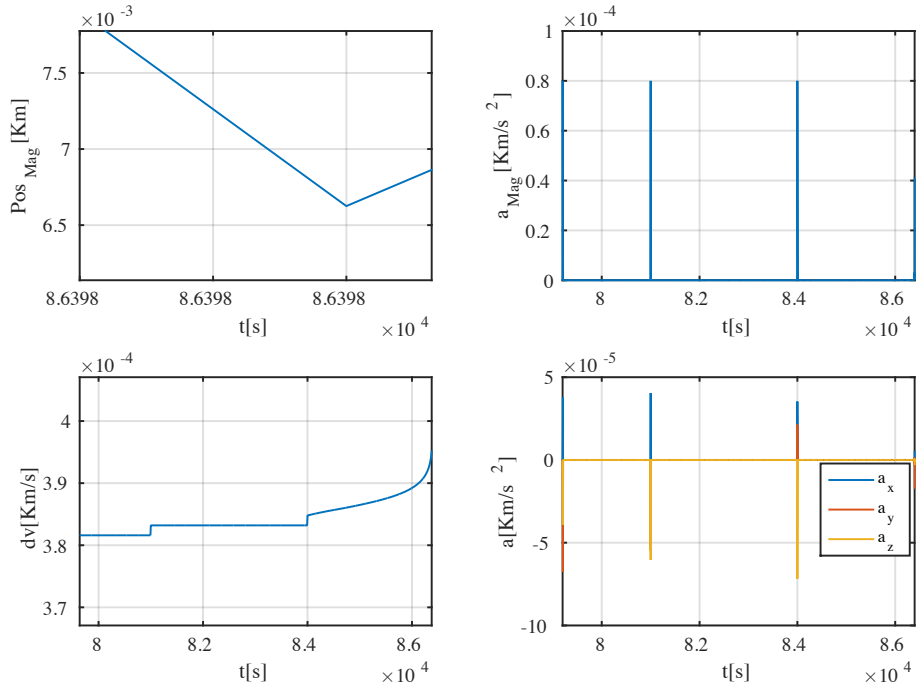


**Figure 9. KI+PN Controller profile: Position magnitude vs. time (top left), Commanded acceleration magnitude vs. time (top right), Total dv usage vs. time(bottom left), and Applied accelerations of KI+PN guidance law applied to an asteroid intercept problem (bottom right)**

distance of 7.01 meters. Pulses were planned at three times which were at 2 hour, 1.5 hour and 40 min before the expected intercept time. As shown in Figure 8, the pulse activated the acceleration commands two times prior to intercept.

Figure 9 presents the computed desired commands, relative position magnitude between the spacecraft and asteroid Bennu of a KI and PN guidance controller hybrid. The hybrid KI and PN controller demonstrated an overall improvement compared to KI, TPPN, as well as PN controllers. Using this hybrid controller scheme resulted in a miss distance of 6.625 meters. The KI controller had preplanned pulses which were between 2 hour and 40 min before the intercept time. After the lower bound of 40 minutes before intercept, the PN controller was activated. Additionally, the pulse was applied three times which were at 2 hour, 1.5 hour and 40 min before the expected intercept time. As expected, the KI controller commanded 2 pulses prior to activating PN guidance.

The second hybrid scheme explored uses KI and TPPN guidance. Figure 10 shows the estimated spacecraft change in velocity for the hybrid KI and TPPN guidance controller. As compared to the all other guidance schemes, the hybrid KI and TPPN controller demonstrated an improvement in expended change in velocity as well as minimum miss distance, which was found to be 5.45 meters. similar to the KI/PN hybrid, the KI controller was first activated between 2 hour and 40 min before the intercept time. However, thereafter the PN controller was activated until minimum relative distance was achieved. Again, the pulse was applied three times which were at 2 hour, 1.5 hour and 40 min before the expected intercept time. The pulse activated the acceleration commands two times as shown in Figure 10.

Figure 11 presents the velocity usage for the guidance controller methods investigated using HIGS software. As shown in the top portion of Figure 11, the KI controller requires more change in velocity compared to the both PN and TPPN. However, this is due to the KI controller always

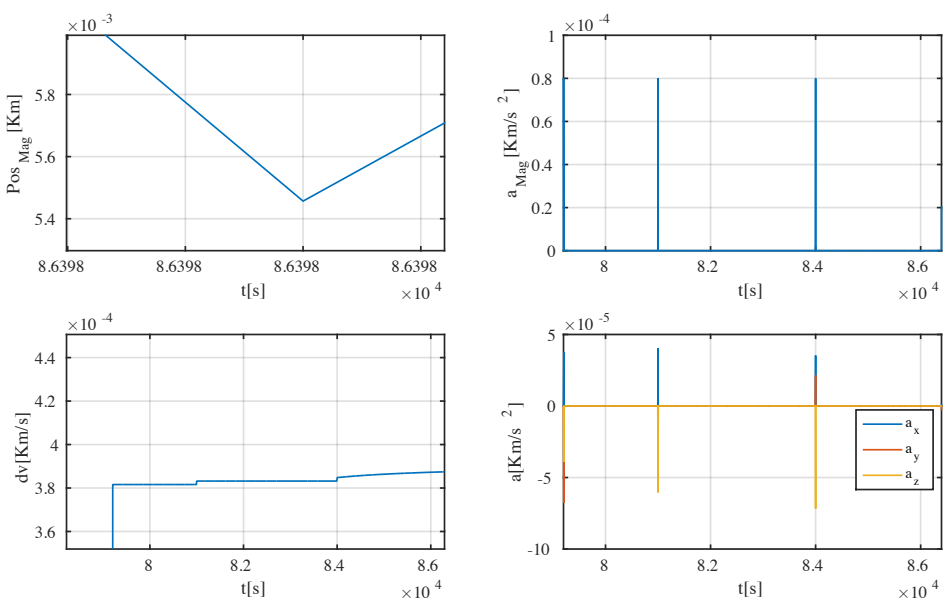


**Figure 10. KI+TPPN Controller profile: Position magnitude vs. time (top left), Commanded acceleration magnitude vs. time (top right), Total dv usage vs. time(bottom left), and Applied accelerations of KI+TPPN guidance law applied to an asteroid intercept problem (bottom right)**

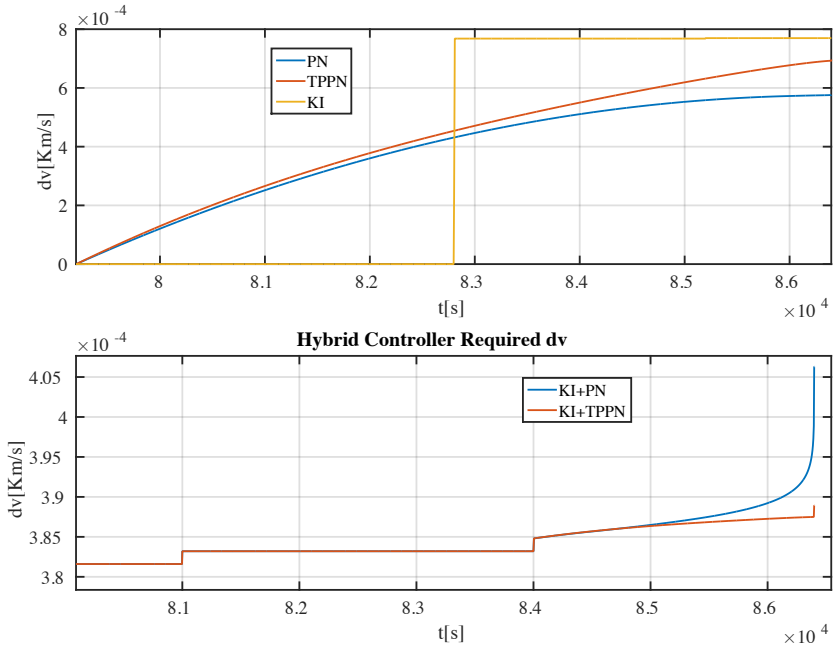


**Figure 11. Compare total dv usage vs. time**

commanding maximum allowable thrust. The PN is the most efficient controller as it requires lesser spacecraft change in velocity. This may be improved by implementing a higher order line of sight rate approximation or a smoothing filter. In the bottom half of Figure 11, each hybrid controller is shown to decrease the velocity change usage by approximately 50 percent. Thus, hybrid controller improves the energy usage as shown in bottom of 11.

## CONCLUSION

In conclusion, we investigated the different guidance controllers that would be applicable to asteroid intercept missions. The controllers were PN, TPPN, and KI. In addition, we analyzed our two proposed hybrid controls, which are the combinations of KI and PN guidance as well as KI with TPPN.

The performance of these controllers has been tested via a developed simulation, HIGS. The simulator considered error sources modeled in the navigation simulation, which was incorporated in the spacecraft initial position and velocity state components. A manipulated Bennu orbit state, that had been modified to impact Earth, used to demonstrated the guidance controllers.

The PN guidance controller performed well to intercept an asteroid that has a size of 50 to 100 meters in diameter. However, PN controller showed non-smooth acceleration commands due to the finite differencing on the computation of the line-of-sight rate. Similarly, the performance of both TPPN and KI controllers were in the required range of intercepting the target asteroid. These two controllers have a smoother command compared to PN. However, they required more spacecraft change in velocity to execute the commands compared to PN.

The noble hybrid approach performance showed an improvement both in the expended velocity change (delta-v) for the propulsion system as well as the minimum miss distance.

The team direction of the future research shall include implementation of other error sources, such as random centroid image pixel noise with bias. In addition, the incorporation of PN and TPPN Schmitt triggers, as well smoothing filters will be investigated.

## ACKNOWLEDGEMENT

This research was supported in part by an appointment to the NASA Mission Directorate Research Participation Program. This program is administered by the Oak Ridge Institute for Science and Education through an interagency agreement between the U.S. Department of Energy and NASA.

## REFERENCES

[1] Hawkins, M., Guo, Y., and Wie, B., Spacecraft Guidance Algorithms for Asteroid Intercept and Rendezvous Missions, Intl J. of Aeronautical & Space Science, Vol. 13 (2), pp. 154169 (2012)

[2] Brent W. Barbee, Bong Wie, Mark Steiner, Kenneth Getzandanner, Conceptual design of a flight validation mission for a Hypervelocity Asteroid Intercept Vehicle, Acta Astronautica, Volume 106, JanuaryFebruary 2015, Pages 139-159, ISSN 0094-5765

[3] Janus, P., John, Homing Guidance (A Tutorial Report) AD-756 973, Space and Missile Systems Organization, 10 December 1964.

[4] Lyzhoft, J.,Hawkins, M., and Wie, B.,GPU-Based Optical Navigation and Terminal Guidance Simulation of a Hypervelocity Asteroid Intercept Vehicle, AIAA-2013-4966, AIAA Guidance, Navigation, and Control Conference, Boston, MA, August 19-22,2013.

[5] Inanc Moran and Turgay Altilar. ”Three Plane Approach for 3D True Proportional Navigation”, AIAA Guidance, Navigation, and Control Conference

[6] Matt Hawkins, Alan Pitz, Bong Wie, and Jesus Gil-Fernandez. ”Terminal-Phase Guidance and Control Analysis of Asteroid Interceptors”, AIAA Guidance, Navigation, and Control Conference,

[7] Vallado, D.A., 2001. Fundamentals of astrodynamics and applications (Vol. 12). Springer Science & Business Media.